ARTICLE OPEN

Check for updates

Sex-specific cortical networks drive social behavior differences in an autism spectrum disorder model

Mariana Lapo Pais[1,2,3], José Sereno[2,3,4], Vanessa A. Tomé[2,5], Carla Fonseca[2,6], Camila Seco[1], Inês Ribeiro[7,8], João Martins[2,3], Ana Fortuna[2,6], Antero Abrunhosa[2,3,5], Luísa Pinto[7,8], Miguel Castelo-Branco[2,3,9] and Joana Gonçalves[2,3,9]✉

Social behavior is highly sensitive to brain network dysfunction caused by neuropsychiatric conditions like autism spectrum disorders (ASDs). Some studies suggest that autistic females show fewer social skill impairments than autistic males. However, the relationship between sex differences in social behavior and sexually dimorphic brain neurophysiology in ASD remains unclear. We hypothesize that sex-specific changes in cortical neurophysiology drive the sexual dimorphism observed in social behavior for ASD. To test this, we used male and female *Tsc2*$^{+/-}$ mice, a genetic ASD model, to examine cortical neuron morphology, the serotonergic system, E/I balance, structural connectivity, and social behavior. At the cellular level, transgenic males had shorter and less complex cortical basal dendrites, while transgenic females showed the opposite in apical dendrites. Notably, only *Tsc2*$^{+/-}$ females exhibited changes in the serotonergic system and E/I balance, with reduced cortical 5-HT$_{1A}$ receptor density and increased excitability. Additionally, activation of these serotonin receptors in transgenic animals correlated with E/I imbalance, highlighting inherent sexual dimorphisms in neuronal connectivity. In parallel, the TSC2 mouse model displayed sex-dependent changes in the structural connectivity of the cortex-amygdala-hippocampus circuit and social behavior: females showed a reduced number of axonal fiber pathways and reduced sociability, while males exhibited a loss of tissue density and deficits in social novelty. Moreover, in our ASD mouse model, better social performance correlated with the cortical serotonergic system. Our findings suggest that sex-dependent alterations in cortical neurophysiology, particularly in the serotonergic system, may contribute to the sexually dimorphic social behaviors observed in ASD.

Translational Psychiatry (2025)15:251 ; https://doi.org/10.1038/s41398-025-03464-7

INTRODUCTION

Autism spectrum disorder (ASD) is a neurodevelopmental condition characterized by social communication difficulties, restricted and repetitive behaviour and sensory anomalies [1] that affects 1 in 36 children [2]. This disorder is frequently diagnosed in males, with evidence suggesting that females are more likely to be misdiagnosed or underdiagnosed [3] and to show significantly better social interaction and communication skills, often referred to as social camouflaging [4, 5]. Despite the strong sexual dimorphism in social behavior for ASD, specific cellular and molecular alterations that might contribute to those distinct manifestations remain unclear.

The imbalance between excitatory and inhibitory (E/I) signaling is the most accepted hypothesis as a mechanism underlying social impairment in ASD [6]. Recently, ASD preclinical and clinical studies have provided evidence that E/I imbalance is heterogeneous both at the intra- and inter-subject [7–9]. Accordingly, it was observed that elevated excitatory activity, specifically in the mouse prefrontal cortex (PFC), results in impaired social behavior [10]. These findings indicated that biological sex interferes with social neuronal networks, especially E/I balance, leading to distinct autistic manifestations. In parallel, the serotoninergic (5-HTergic) system has also been recognized as a critical player in shaping social responses [11]. Actually, high 5-HT levels are associated with increased sensitivity to social factors [12]. Accordingly, enhancing 5-HT activity reverses impairments in sociability across multiple mouse models for ASD [13]. Strangely, despite well-known differences in the 5-HT signalling between males and females, including the rate of synthesis and receptor binding [14], sex as a biological variable is not included in most studies. Importantly, a study showed that although the 5-HTergic system significantly regulates social behavior in both males and females, its influence is more pronounced in females, particularly under stress-like conditions [15]. However, the role of the 5-HTergic system and E/I balance in the sex-specific social deficits observed between males and females with ASD remains poorly understood.

At the cellular level, both E/I balance and 5-HTergic are preserved through precise synaptic connections [16, 17]. The inherent morphology of neurons, including dendritic arborisations and dendritic spines, stands as a pivotal determinant for neuronal

[1]University of Coimbra, Faculty of Sciences and Technology, Coimbra, Portugal. [2]University of Coimbra, Coimbra Institute for Biomedical Imaging and Translational Research (CIBIT), Coimbra, Portugal. [3]University of Coimbra, Institute for Nuclear Sciences Applied to Health (ICNAS), Coimbra, Portugal. [4]University of Coimbra, CQC-IMS, Chemistry Department, Coimbra, Portugal. [5]ICNAS Pharma, University of Coimbra, Coimbra, Portugal. [6]University of Coimbra, Laboratory of Pharmacology, Faculty of Pharmacy, Coimbra, Portugal. [7]Life and Health Sciences Research Institute (ICVS), School of Medicine, University of Minho, Braga, Portugal. [8]ICVS/3B's - PT Government Associate Laboratory, Braga/Guimarães, Portugal. [9]University of Coimbra, Institute of Physiology, Faculty of Medicine, Coimbra, Portugal. ✉email: jgoncalves@icnas.uc.pt

Received: 24 September 2024 Revised: 7 May 2025 Accepted: 30 June 2025
Published online: 21 July 2025

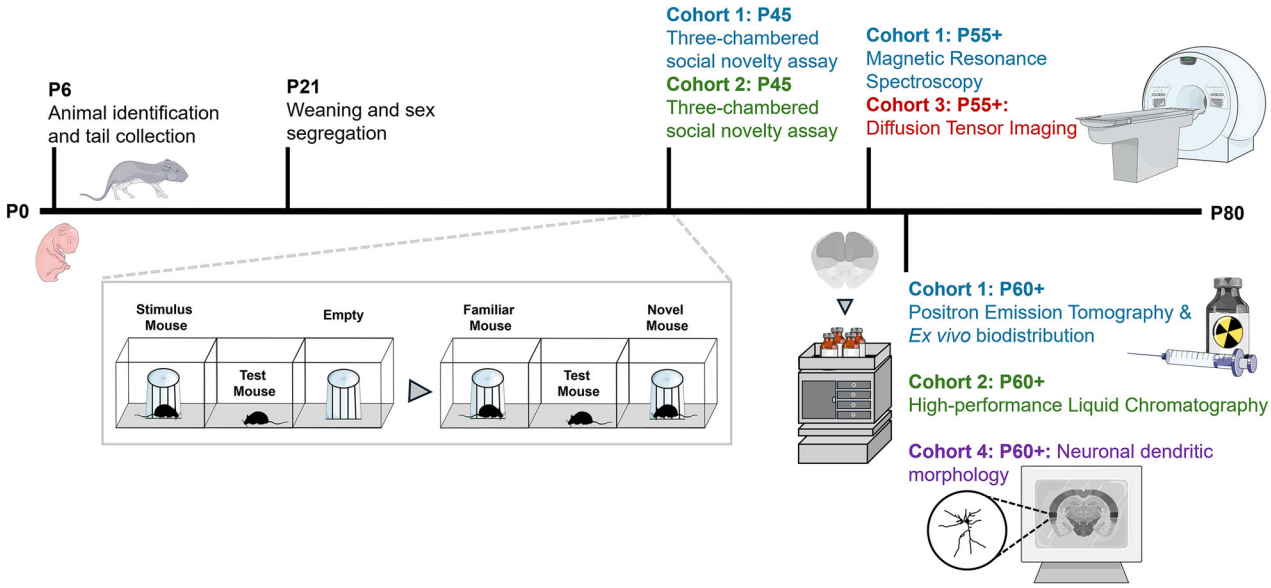

Fig. 1 Timeline of all experiments and different cohorts in this study. Animals were identified on P6, and tail tips were collected for posterior genotyping. All pups were housed together with the dam until P21 and segregated by sex from P21 onwards. The three-chamber social novelty assay behavioral test was conducted at P45 for a dataset of cohorts 1 and 2 ($n = 12$ mice per group). A dataset of cohort 1 undergone in vivo ^{1}H-MRS (P55 +; $n = 9$–12 mice per group), in vivo PET imaging (P60 +; $n = 4$–5 mice per group) and ex vivo biodistribution (P60 +; $n = 7$–8 mice per group). In parallel, a dataset of cohort 2 underwent HPLC analysis (P60 +; $n = 13$–15 mice per group). Lastly, in vivo DTI (P55 +; $n = 10$–14 mice per group) and Golgi staining for neuronal morphological analyses (P60 +; $n = 4$–5 mice per group) were conducted for cohort 3 and 4. ^{1}H-MRS Proton Magnetic Resonance Spectroscopy, HPLC High-Performance Liquid Chromatography, DTI Diffusion Tensor Imaging, P Postnatal day, PET Positron Emission Tomography. The figure was partly generated using Allen Mouse Brain Atlas, atlas.brain-map.org, and Servier Medical Art, provided by Servier, licensed under a Creative Commons Attribution 3.0 unported license.

connectivity [18, 19]. The neocortex circuitry is organised to allow associative processing by comparing local inputs and long-range inputs [20], making it crucial to characterize abnormalities in both basal (integrate inputs from local circuits) and apical (typically process signals from distant brain regions) dendrites to establish a more comprehensive understanding of neural functions [20, 21]. Alterations in both morphological and molecular signaling can disrupt the typical development of structural and functional neural networks, potentially contributing to the clinical manifestations of some neuropsychiatric diseases [22]. In fact, data on distinct psychiatric disorders often linked symptoms such as social and cognitive impairments and emotional dysregulation to dysfunction within the cortex-hippocampal network [23–26]. Further, this overlap has also been suggested to be influenced by the network's sensitivity to stress and its strong connection with the amygdala [26]. Based on that evidence, we hypothesized that cortical neurophysiological alterations in ASD can lead to network impairments in structural connectivity involving the cortex-amygdala-hippocampus circuit, which might be implicated in the pathophysiology of TSC.

At last, numerous pieces of convergent evidence collected from studies of humans and rodents suggested that the PFC plays a pivotal role in social interactions [23–25]. Accordingly, frontal cortical activity, explicitly involving the serotoninergic system, is crucial for regulating social, cognitive, and emotional functions [27, 28] as inhibitory (GABAergic) and excitatory (glutamatergic) transmission [29]. The distinct differences in ASD-related social skills between males and females underscore the critical need to explore the sexually dimorphic mechanisms underlying their molecular basis. Based on all the above-mentioned evidence, we hypothesized that cortical morphological and neurophysiological alterations linked to the serotonergic system may impact structural connectivity and be pivotal in the social impairments seen in ASD. By addressing this gap, our study could provide valuable insights into the sex-specific manifestations of ASD.

MATERIALS AND METHODS

Animals

Heterozygous *Tsc2*$^{+/-}$ mice with C57BL/6N background were crossed with C57BL/6J wild-type (WT) mice to generate experimental animals as previously described [30]. The *Tsc2*$^{+/+}$ littermates were used as controls and referred to as wild-type (WT). Mice were housed at the Institute of Nuclear Science Applied to Health (ICNAS) animal facility at 22 °C under a 12-h light-dark cycle and provided ad libitum access to food and water. All experimental procedures were reviewed and approved by the Animal Welfare and Ethics Body of ICNAS (8/2023) following the guidelines of the European Community for the use of animals in the laboratory (86/609/EE) and the Portuguese law for the care and use of experimental animals (DL n° 129/92). A timeline of all experiments and different cohorts is represented in Fig. 1. All experiments were conducted and analyzed by an operator blinded to sex and genotype, with no randomization applied.

Neuronal dendritic morphology

Golgi-cox staining. Mice were anaesthetized intraperitoneally (i.p.) with a mixture of ketamine (200 mg/Kg) and xylazine (16 mg/Kg), followed by intracardiac perfusion with 0.9% sodium chloride (NaCl) solution (pH 7.3). Brains were carefully removed, immersed in Golgi-Cox solution, and kept in the dark for 15 days. Next, they were transferred to a 30% sucrose solution and kept in the refrigerator in the dark for 2–5 days. Coronal sections (200 µm) were obtained in a vibratome (Leica VT100S, Germany), collected in 6% sucrose and blotted dry onto gelatin-coated microscope slides. Brain sections were subsequently alkalinised in 18.7% ammonia, developed in Dektol (Kodak), fixed in Kodak Rapid Fix, dehydrated and xylene cleared before coverslipping.

Morphological analysis. Cortical regions were delineated based on the Allen Mouse Brain Atlas (atlas.brain-map.org) and pyramidal neurons were selected based on their cytoarchitecture, including a clear identifiable axon and apical dendrite. Dendritic arbors of selected neurons were traced at 100x (oil) magnification using a motorised microscope (BX51, Olympus) and Neurolucida software (Microbrightfield Version 2022, MBF Bioscience) with the AutoNeuron extension module. For each animal, 10 neurons were reconstructed, and a three-dimensional analysis of the reconstructed neurons was performed. Spines were studied in segments of 30 µm in the apical branch and classified into spine type. Spine percentages were calculated as (number of spines per type)/(total number of spines).

In vivo imaging studies
Animals were anaesthetised using 1.5–2% isoflurane during acquisitions. Magnetic resonance (MR) and positron emission tomography (PET) acquisitions were performed on a 9.4T MR preclinical scanner (Bruker Biospec, Billerica MA) operated with ParaVision (v6.0.1) and on a MicroPET scanner based on resistive plate chamber detectors (RPC-PET) [31], respectively. Detailed description of MR imaging data acquisition methodology can be found in the Supplementary File.

^{1}H-magnetic resonance spectroscopy
For localized proton magnetic resonance spectroscopy (^{1}H-MRS), data were collected in a volume of interest placed on the prefrontal cortex (PFC). Spectra analysis was performed using linear combination modeling LCModel (Stephen Provencher Inc., Toronto, ON, Canada) [32]. Metabolite quantification was performed by applying the internal water reference method. The Cramer–Rao lower bounds (CRLB) under 20% for glutamate and 30% for γ-aminobutyric acid (GABA) were used as a reliability measure of the metabolite concentration estimation [33].

[carbonyl-^{11}C]WAY-100635 positron emission tomography
[*carbonyl*-^{11}C]WAY-100635 was synthesized according to a published method described in [34], with some modifications to fit into the commercial radiosynthesis modules housed at ICNAS Pharma Unipessoal, Lda (Coimbra, Portugal). Detailed [*carbonyl*-^{11}C]WAY-100635 radiosynthesis description can be found in the Supplementary File.

Acquisition. The radiotracer, [carbonyl-^{11}C]WAY-100635 PET, a selective 5-HT$_{1A}$ antagonist radiotracer, was administered intravenously (i.v.) in a total injected activity of ~10 uCi/g. Approximately 5 min after tracer injection, a 50-min list mode data was initiated. The bed had fiducial marks installed to align the PET image with Magnetic resonance imaging (MRI).

Quantification. Quantitative imaging was performed using PMOD (PMOD, v3.6; PMOD Technologies, Zürich, Switzerland, RRID:SCR_016547). PET images were co-registered with the anatomical MRI, and a volume of interest (VOI) including the whole cortex was used based on an integrated anatomical ATLAS (Ma-Benveniste-Mirrione) [35]. The percentage of injected dose per VOI volume (%ID/mL) was calculated as [[total positron (β+ radioactivity) concentration in the VOI (Bq/mL)]/[total positron (β+ radioactivity) injected (Bq)]*100] from 30–50 min post-injection. Additionally, the standardised uptake value (SUV) was calculated as [[total positron (β+ radioactivity) concentration in the VOI (Bq/mL)]/[total positron (β+ radioactivity) injected (Bq)/body weight (g)]] from 30-50 min post-injection. The SUV ratio (SUVr) is calculated by dividing the SUV in the target region by the SUV in the cerebellum (reference region).

Ex vivo biodistribution of [carbonyl-^{11}C]WAY-100635
Animals were injected with [carbonyl-^{11}C]WAY-100635 intravenously (i.v.) in a total injected activity of ~10 uCi/g. After 50 min, a cardiac perfusion with saline solution was done to clean out all circulating blood, and ex vivo biodistribution (percentage of injected dose per tissue weight, %ID/g of tissue) was performed by gamma counting (CRC® – 55 tW radioisotope dose calibrator, Capintec, Ramsey, NJ, USA) in the PFC.

High-performance liquid chromatography
Animals were euthanized, and PFC samples were collected and stored at −80 °C. Tissues were homogenized in ice-cold 0.2 M perchloric acid with 6 mM Cysteine and centrifuged for 15 min at 4147 × g at 4 °C. The supernatant was then deproteinised with 2.0 M perchloric acid and centrifuged for 4 min at 20817 × g at 4 °C. Following tissue preparation, tryptophan (tryp) and 5-HT were quantified with a Shimadzu high-performance liquid chromatography (HPLC) system (Shimadzu Corporation, Kyoto, Japan), constituted by a solvent delivery unit (LC-20A), a degasser system (DGU-20A5), an autosampler (SIL-20AHT), a column oven (CTO-10ASVP) and a fluorescence detector ((RF-20AXS). Chromatographic separations were performed based on the previous validated method [36].

Diffusion tensor imaging
Each diffusion tensor image (DTI) acquisition consisted of 22 slices, 0.5 mm thick, encompassing the entire brain. DTI data were post-processed using TrackVis and Diffusion Toolkit (Ruopeng Wang, Van J. Wedeen, TrackVis.org, Martinos Center for Biomedical Imaging, Massachusetts General Hospital). For each acquisition, an anatomical ATLAS including whole cortex, amygdala and hippocampus was generated from the anatomical MRI and using PMOD (PMOD, v3.6; PMOD Technologies, Zürich, Switzerland, RRID:SCR_016547) integrated anatomical ATLAS, Mouse (Ma-Benveniste-Mirrione) [35]. Tract-based analysis was performed for the cortex, amygdala and hippocampus to obtain the total fibers number, the fractional anisotropy (FA) and the apparent diffusion coefficient (ADC) values.

Three-chambered social novelty test
Each test animal was placed in the three-chamber test arena [37] in a red-light environment (7 LUX). The assay consisted of two phases, the first to study social interaction and the second to study social novel interaction, after a 10-min habituation period with two empty wire cages (Empty) in the side chambers.

Sociability test phase (first phase): a cage with an unfamiliar mouse (social stimulus) was introduced to one side, and the test mouse was allowed to explore all three chambers freely for 10 min.
Social novelty test phase (second phase): the empty wire cage was replaced with a cage with another unfamiliar mouse (novel stimulus). The subject was allowed to explore all three chambers for 10 min.

Unfamiliar mice were age- and sex-matched and previously habituated to the wire cages. Locomotory metrics were examined from top-video recordings using the Tracking (SMART) video system (v2.5; Panlab S.L., Spain). Total time sniffing social and novel stimulus was manually quantified. The social and social novel indexes for each animal were respectively calculated as [Social index = ((Social-Empty))/((Social + Empty))] and [Social Novel index = ((Novel-Familiar))/((Novel + Familiar))], each variable referring to the total time sniffing the respective stimulus.

Statistical analysis
Sample size was defined to ensure adequate power within acceptable limits while minimizing animal use according to [E = Total number of animals – Total number of groups; any sample size, which keeps E between 10 and 20 was considered as adequate] [38]. Statistical analyses were performed using GraphPad Prism version 8.0.1 (GraphPad Software, San Diego, California) and R studio (Integrated Development Environment for R. Posit Software, PBC, Boston, MA). Results are presented as mean values ± standard error of mean (SEM), with similar variance between groups. All datasets were tested for normality with the Shapiro–Wilk test. For non-parametric data, quantile-quantile (Q-Q) plots were evaluated, and parametric tests were used as observations lay approximately on the straight line of the Q-Q plot. Analyses of variance (ANOVA) with Sidak's test were used for multiple comparisons. The Pearson correlation, or the non-parametric alternative Spearman correlation, was computed to assess the relationship between multiple variables. Three-dimensional Sholl analysis was used to evaluate the spatial arrangement of dendritic material by quantifying the number of dendritic intersections at concentric 10-µm intervals from the soma by 2WAY ANOVA repeated measures with Sidak's test for multiple comparisons. Outliers were removed using the ROUT method (Q = 5%).

RESULTS
Tsc2$^{+/-}$ animals exhibit sexual-dependent alterations in cortical neurons, affecting both basal and apical dendrites
Neuronal morphology and complexity of cortical dendritic arborization were assessed as indirect indicators of connectivity at the cellular level (Fig. 2). We reveal that genotype significantly influenced relevant neuronal morphological measures (soma area: $F(1, 171) = 11.09$, $p < 0.01$, Fig. 2B; number of dendrites: $F(1, 174) = 10.13$, $p < 0.01$, Fig. 2C), which can impact synaptic connectivity in *Tsc2*$^{+/-}$ animals. Moreover, we exposed a significant interaction between genotype and sex (soma area: $F(1, 171) = 8.906$, $p < 0.01$, Fig. 2B) and sex-dependent changes after the post hoc tests analysis. Specifically, we exposed that transgenic males exhibit neuronal changes reflected by reduced soma areas ($p < 0.01$, Fig. 2B) and decreased dendritic complexity (number of dendrites: $p = 0.04$, Fig. 2C) compared with WT group.

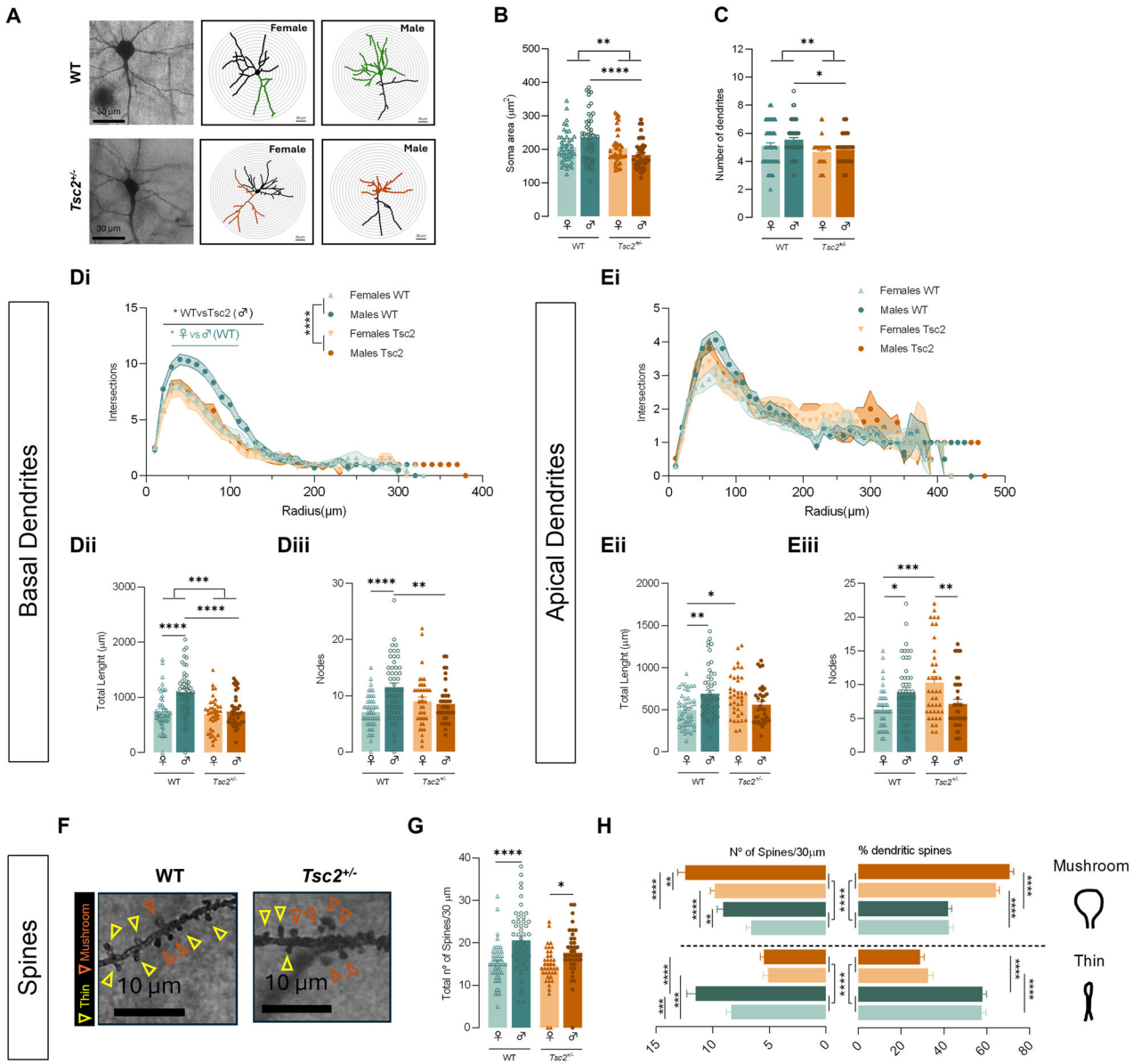

Fig. 2 ***Tsc2*$^{+/-}$ animals exhibit sexual-dependent alterations in cortical neurons for both basal and apical dendrites. A** Representative images of cortical pyramidal neurons labelled with Golgi-Cox and corresponding 3D reconstructions with soma and basal dendrites and apical dendrites highlighted with colour (green for WT and orange for *Tsc2*$^{+/-}$) for males and females, respectively. Several aspects of dendritic morphology were examined, including soma area (µm^2) **B** and number of dendrites **C** for each genotype and sex. Moreover, basal dendrites intersections **Di**, total length (µm) **Dii** and nodes **Diii** and apical dendrites intersections **Ei**, total length (µm) **Eii** and nodes **Eiii** were accessed separately. **F** Representative images of dendritic spines of cortical neurons labelled with Golgi-Cox for WT and *Tsc2*$^{+/-}$ mice. **G** The total number of spines was quantified in segments of 30 µm. Spines in the selected segments were classified into spine type, mushroom (top) and thin (bottom) and evaluated according to their **H**, left total number and **H**, right relative percentage. Data plotted as individual neuron values (dots) and mean ± SEM (columns and bars). Number of cells: 35–50 in $N = 4$–5 mice. *$p < 0.05$, **$p < 0.01$, ***$p < 0.001$, ****$p < 0.0001$ by 2WAY ANOVA with Sidak's multiple comparisons-test **B, C**; **Dii**-**Diii**; **Eii**-**Eiii**; **G, H**. Three-dimensional Sholl analysis was used to evaluate the spatial arrangement of dendritic material by quantifying the number of dendritic intersections at concentric 10-µm intervals from the soma by 2WAY repeated measures ANOVA with Sidak's multiple comparisons-test **Di**; **Ei**. The figure was partly generated using Allen Mouse Brain Atlas, atlas.brain-map.org.

Then, we characterize basal and apical dendrites separately and exposed that only basal dendrites were significantly influenced by genotype (intersections: $F(1, 176) = 18.96$, $p < 0.01$, Fig. 2Di; total length: $F(1, 173) = 15.84$, $p < 0.01$, Fig. 2Dii) and sex (intersections: $F(1, 176) = 11.00$, $p < 0.01$, Fig. 2Di; total length: $F(1, 173) = 14.60$, $p < 0.01$, Fig. 2Dii; nodes: $F(1, 173) = 9.691$, $p < 0.01$, Fig. 2Diii). However, an interaction between genotype and sex on both basal and apical dendrites was reported (basal intersections: $F(1, 176) = 7.120$, $p < 0.01$, Fig. 2Di; total basal length: $F(1, 173) = 8.646$, $p < 0.01$, Fig. 2Dii; basal nodes: $F(1, 173) = 15.07$, $p < 0.01$, Fig. 2Diii; total apical length: $F(1, 163) = 14.60$, $p < 0.01$, Fig. 2Eii; apical nodes: $F(1, 171) = 18.88$, $p < 0.01$, Fig. 2Eiii). Moreover, post hoc tests showed that basal arbors from transgenic male mice were less complex (intersections specifically proximal to soma: $p < 0.05$, Fig. 2Di; nodes: $p < 0.01$, Fig. 2Diii) and shorter (total length: $p < 0.01$, Fig. 2Dii) compared with WT males. In contrast, we showed that the apical dendritic arbors of transgenic females occupied higher regions (total length:

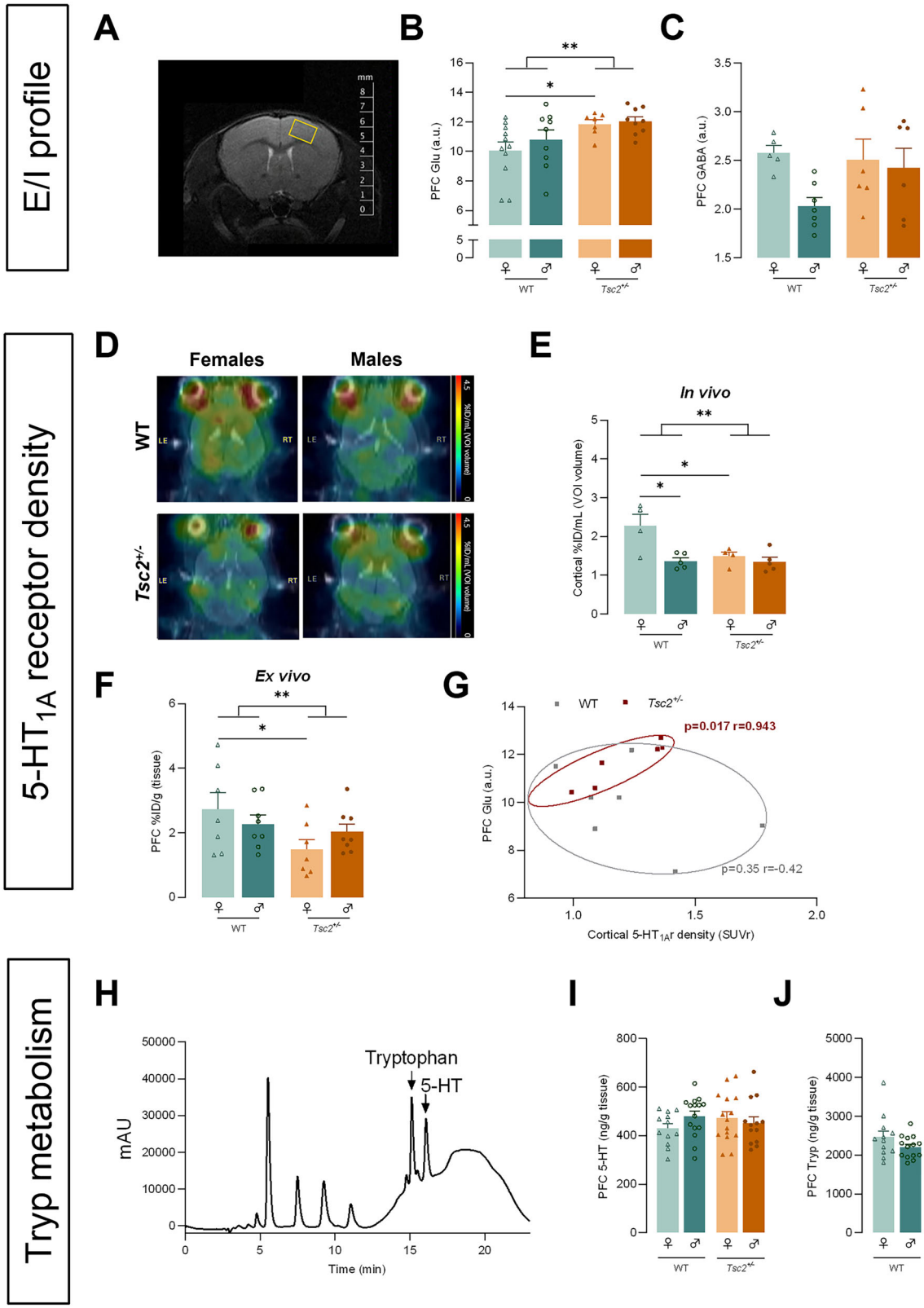

$p = 0.01$, Fig. 2Eii) and displayed increased complexity (nodes: $p < 0.01$, Fig. 2Eiii) than those of WT females.

Furthermore, several sexual dimorphisms were reported specifically for control group. WT males presented increased dendritic complexity (basal intersections proximal to soma: $p < 0.05$, Fig. 2Di; basal nodes: $p < 0.01$, Fig. 2Diii; apical nodes: $p = 0.02$, Fig. 2Eiii) and larger arbor sizes (total basal length: $p < 0.01$, Fig. 2Dii; total apical length: $p < 0.01$, Fig. 2Eii) than WT females. In contrast, for transgenic mice, $Tsc2^{+/-}$ males exhibited less complex apical dendrites compared with transgenic females (nodes: $p < 0.01$, Fig. 2Eiii).

Fig. 3 Sex-specific changes in the cortical serotonergic system were strongly correlated with glutamate concentrations in *Tsc2*$^{+/-}$ mice. **A** Representative MRI image with MRS voxel (yellow square) localisation in the PFC. E/I balance was accessed from **B** in vivo PFC Glu concentration (a.u.) and **C** GABA concentration (a.u.) for each genotype and sex. **D** Representative MRI/PET in vivo neuroimage of [carbonyl-^{11}C]WAY-100635. 5-HT$_{1A}$ receptor density was accessed from **E** in vivo cortical %ID/g (body weight) and **F** ex vivo PFC %ID/g (tissue) for each genotype and sex. **G** Correlation between PFC Glu concentration (a.u.) and cortical 5-HT$_{1A}$ receptor density (SUVr) for each genotype. **H** Representative chromatogram of PFC samples collected from control mice. PFC concentrations (ng/g tissue) of **I** 5-HT and **J** tryp for each genotype and sex. The results are expressed as mean ± SEM [$n = 5$–11 **B, C,** $n = 4$–5 **E,** $n = 7$–8 **F,** $n = 6$–7 **G,** $n = 13$–15 **I, J** for each group]. *$p < 0.05$, **$p < 0.01$ by 2WAY ANOVA with Sidak's multiple comparisons-test **B, C, E**–**G, I, J** and Pearsons's correlation (G). %ID/mL Percentage of Injected Dose per mL, 5-HT Serotonin, a.u. arbitrary units, Glu Glutamate, MRI Magnetic Resonance Imaging, MRS Magnetic Resonance Spectroscopy, PET Positron Emission Tomography, PFC Prefrontal Cortex, ROI Region Of Interest, Tryp tryptophan.

Finally, to further evaluate synaptic connectivity, spines were quantified (Fig. 2F–H). Our results exposed that number of spines were only significantly influenced by sex ($F(1, 171) = 32.81$, $p < 0.01$, Fig. 2G) and not by genotype. In specific, males exhibited a higher number of spines compared with females in both transgenic ($p = 0.0487$, Fig. 2G) and control ($p < 0.01$, Fig. 2G) groups. Segregation by mushroom (mature) and thin (immature) spines revealed a significant effect of genotype on spine number (Thin: $F(1, 170) = 66.86$, $p < 0.01$; Mushroom: $F(1, 174) = 42.58$, $p < 0.01$, Fig. 2H) and their relative percentage (Thin: $F(1, 170) = 177.3$, $p < 0.01$; Mushroom: $F(1, 166) = 179.0$, $p < 0.01$, Fig. 2H). Moreover, we reported sexual dependent changes in spine number, reflect by a significant effect of sex (Thin: sex- $F(1, 170) = 9.688$, $p < 0.01$; Mushroom: sex- $F(1, 174) = 25.63$, $p < 0.01$, Fig. 2H) and interaction between genotype and sex (Thin: $F(1, 170) = 6.031$, $p = 0.02$, Fig. 2H) for this measure. Post hoc tests indicated that transgenic male and female mice exhibited lower number and relative percentage of thin spines ($p < 0.01$, Fig. 2H) but higher number and relative percentage of mushroom spines ($p < 0.01$, Fig. 2H) comparing to their correspondent control group. Moreover, sex-specific alterations were consistent across both WT and transgenic groups, with male mice exhibiting a higher number of spines compared to females ($p < 0.01$, Fig. 2H).

Sex-specific changes in the cortical serotonergic system were strongly correlated with glutamate concentrations in *Tsc2*$^{+/-}$ mice

After assessing cortical neuronal morphology, we evaluate PFC E/I profiles using in vivo ^{1}H-MRS (Fig. 3A–C). Cortical E/I profile analysis revealed a significant effect of genotype for glutamate concentrations ($F(1, 32) = 8.35$, $p < 0.01$, Fig. 3B) and post hoc tests exposed that only *Tsc2*$^{+/-}$ females exhibited significantly higher excitability than their WT littermates ($p < 0.05$, Fig. 3B). For the GABA concentrations (Fig. 3C) and Glu/GABA ratio (Figure S1, Supplementary File), we did not report any significant effect on genotype or sex.

Then, functional changes in the serotonergic system, particularly 5-HT$_{1A}$ receptor density, were assessed using in vivo neuroimaging with [carbonyl-^{11}C]WAY-100635 (Fig. 3D, E). For [carbonyl-^{11}C]WAY-100635 binding, we reported, once again, a significant influence of genotype, sex (genotype – $F(1, 14) = 5.79$, $p = 0.03$; sex - $F(1, 14) = 9.767$, $p < 0.01$, Fig. 3E) and their interaction ($F(1, 14) = 5.235$, $p = 0.04$, Fig. 3E). Post hoc analyses further revealed that only *Tsc2*$^{+/-}$ female mice had lower cortical 5-HT$_{1A}$ receptor density compared with WT group ($p = 0.04$, Fig. 3E). A sexual dimorphism for control animals was also reported reflecting an increased binding in females ($p = 0.01$, Fig. 3E). Considering that receptor binding is also coupled to the delivery of the radiotracer from the vascular space to the cellular target, we also performed ex vivo analysis after circulating blood clearance. From ex vivo biodistribution, only genotype significantly influenced the uptake of radioligand ($F(1, 26) = 4.793$, $p = 0.04$, Fig. 3F). According to the in vivo results, once again, only transgenic female mice had a significantly lower uptake of [carbonyl-^{11}C]WAY-100635 compared with their WT littermates ($p = 0.04$, Fig. 3F). Since the same animals underwent to PET imaging and ^{1}H-MRS [WT: $n = 7$ (3 females and 4 males); *Tsc2*$^{+/-}$: $n = 6$ (3 females and 3 males)], we tested the association of these receptor and neurotransmitter measures (Fig. 3G) and found a strong positive correlation between cortical 5-HT$_{1A}$ receptor density (SUVr) and glutamate concentrations (Spearman correlation; $p = 0.02$; $r = 0.943$, Fig. 3G) only in *Tsc2*$^{+/-}$ animals.

Next, we analyze 5-HT levels and its biochemical precursor, tryptophan, in the PFC using HPLC, providing reliable indicators of 5-HT dysfunction and substrate availability for synthesis (Fig. 3H–J). Interestingly, our analysis of PFC revealed that while control and transgenic mice had similar 5-HT levels for both sexes (Fig. 3I), it was observed that sex significantly influenced tryp concentrations ($F(1, 46) = 10.19$, $p < 0.01$, Fig. 3J). *Tsc2*$^{+/-}$ female mice presented significantly higher tryp levels than transgenic males from post hoc test analysis ($p < 0.05$, Fig. 3J).

Tsc2$^{+/-}$ mice exhibited altered structural connectivity involving the cortex-amygdala-hippocampus circuit in a sex-dependent matter

Given that morphological changes may compromise brain structure and communication between regions, we explored potential alterations in structural connectivity between the cortex and other key networks, such as the amygdala and hippocampus, linked to the pathophysiology of several psychiatric diseases [26] (Fig. 4). Our analysis of structural connectivity for the cortex-amygdala-hippocampus circuity revealed a significant interaction between genotype and sex in apparent diffusion coefficient (ADC) values ($F(1, 43) = 4.579$, $p = 0.0381$, Fig. 4D) and the number of fibers ($F(1, 42) = 5.299$, $p = 0.0264$, Fig. 4E). Interestingly, *Tsc2*$^{+/-}$ male mice presented significantly higher ADC values than WT males ($p = 0.0438$, Fig. 4D), while transgenic females exhibited fewer fibers than their control littermates ($p = 0.0266$, Fig. 4E).

Tsc2$^{+/-}$ mice exhibited sex-specific social deficits strongly correlated with tryptophan metabolism

To investigate social interaction, a three-chambered social novelty test was performed (Fig. 5). From both phases we found a significant interaction between genotype and sex (social index: $F(1, 39) = 8.724$, $p < 0.01$, Fig. 5B; social novel index: $F(1, 42) = 4.889$, $p = 0.03$, Fig. 5E) and a significant influence of genotype for the total distance traveled (sociability phase: $F(1, 44) = 4.980$, $p = 0.03$, Fig. 5C; social novelty phase: $F(1, 44) = 7.624$, $p < 0.01$, Fig. 5F).

Post hoc test analysis further revealed that, transgenic females had higher social deficits during first phase while both locomotory and social alterations were particularly noticeable among transgenic males during second phase. Specifically, *Tsc2*$^{+/-}$ females had a lower social index compared with WT females ($p = 0.02$, Fig. 5B) and *Tsc2*$^{+/-}$ males ($p < 0.01$, Fig. 5B). Moreover, only transgenic male mice displayed lower social novelty preference for the novel stimulus ($p = 0.05$, Fig. 5E) and increased total distance traveled ($p = 0.01$, Fig. 5F), compared with their WT littermates. Interestingly, for all groups, time spent in the social chamber was not significantly correlated with time spent sniffing the social stimulus (Pearson correlation, Fig. 5G), which can be attributed to the

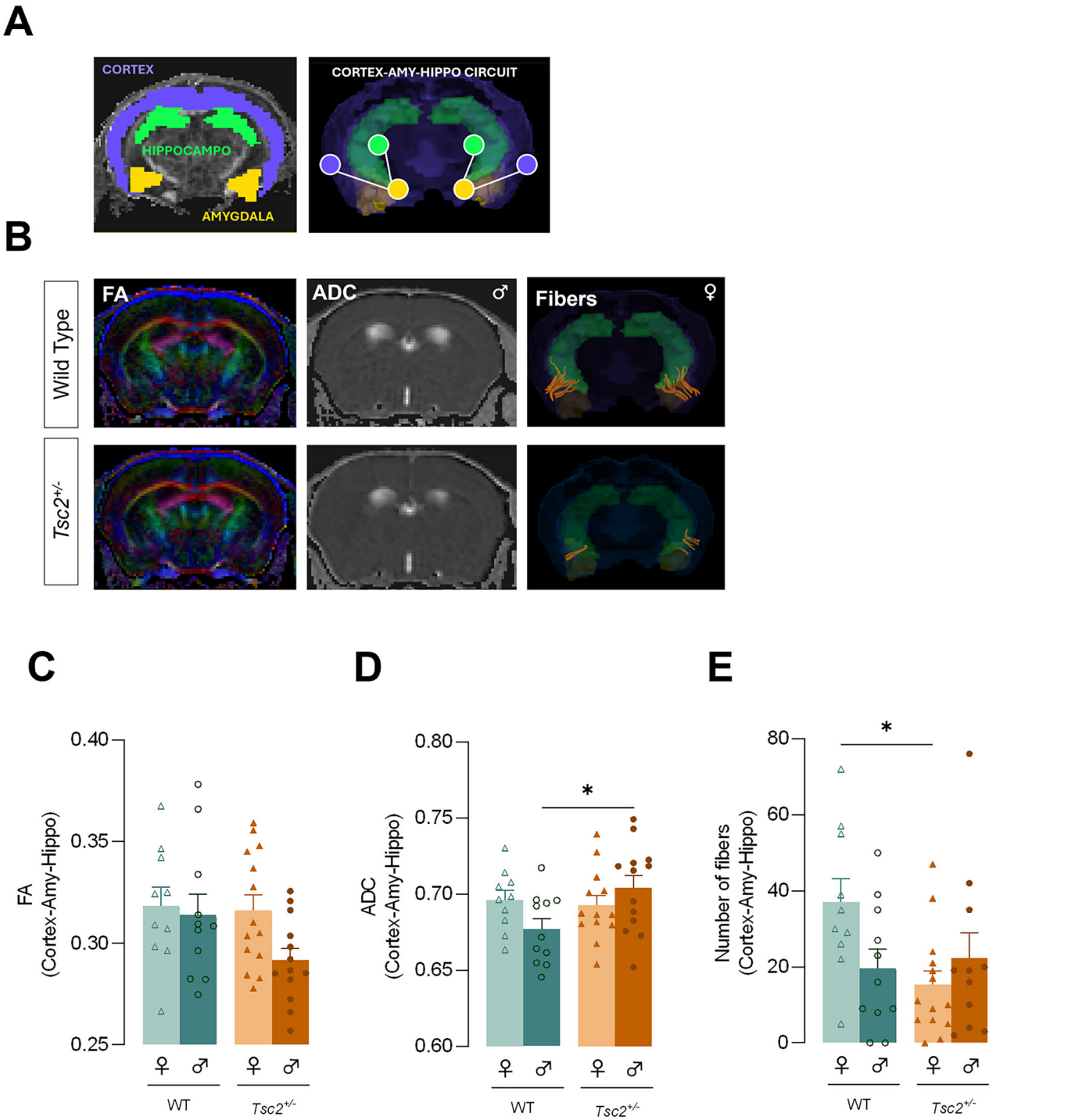

Fig. 4 ***Tsc2***$^{+/-}$ **mice exhibited altered structural connectivity involving the cortex-amygdala-hippocampus circuit in a sex-dependent matter. A** Representative ROI masks for the whole cortex (purple), amygdala (yellow) and hippocampus (green) and a schematic diagram of the cortex-amygdala-hippocampus circuit. **B** Representative images for both WT and *Tsc2*$^{+/-}$ mice of FA color maps, ADC images, and fiber tracts from the sex with the most reported alterations. Structural connectivity measures included **C** FA and **D** ADC values and **E** the number of fiber tracts within the cortex-amygdala-hippocampus circuit. The results are expressed as mean ± SEM ($n = 10$–14 for each group). *$p < 0.05$ by 2WAY ANOVA with Sidak's multiple comparisons test. ADC Apparent diffusion coefficient, AMY Amygdala, FA Fractional anisotropy, HIPPO Hippocampus, ROI Region of interest.

unfamiliarity with the environment. In contrast, the time spent in the social novel chamber was significantly positively correlated with the time spent sniffing the novel stimulus in WT females (Pearson correlation, $p < 0.01$, $r = 0.79$, Fig. 5G), and showed a trend toward significance in WT males (Pearson correlation, $p = 0.08$, $r = 0.59$, Fig. 5G). In *Tsc2*$^{+/-}$ mice, a significant positive correlation was observed only in females (Pearson correlation, $p = 0.02$, $r = 0.65$, Fig. 5G).

Correlation analysis between social behavior and HPLC data (WT: $n = 8$; *Tsc2*$^{+/-}$: $n = 6$) showed that 5-HT and tryp concentrations were positively correlated with social index and social novel index in transgenic animals, respectively (Pearson correlation,

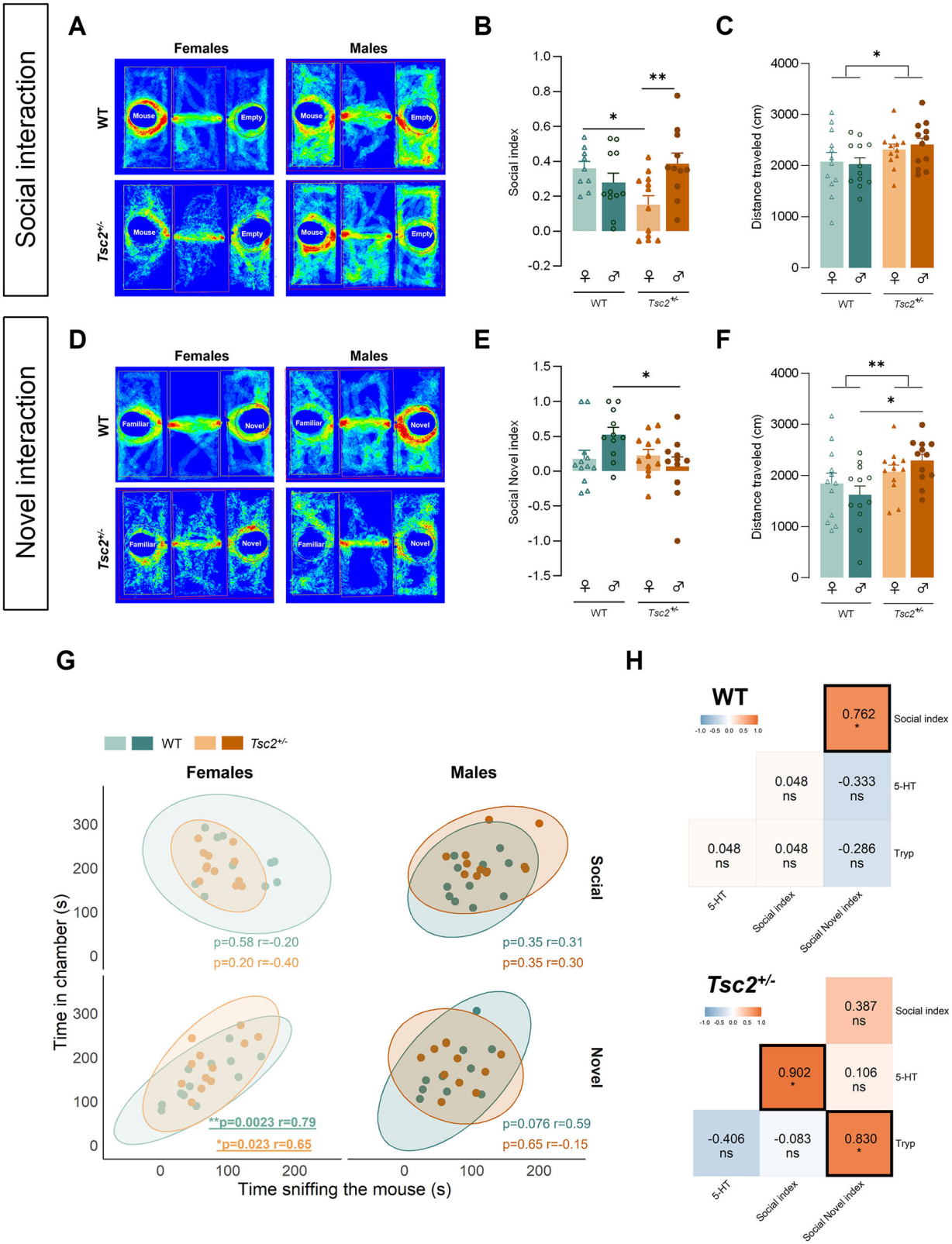

Fig. 5 ***Tsc2*$^{+/-}$ mice exhibit sex-dependent impairment in social behavior strongly correlated with Tryp and 5-HT PFC levels. A, D** Representative locomotory images for the sociability and social novelty test phases. Behavioral measures were examined for sociability phase, including **B** social index and **C** total distance traveled (cm) and social novelty phase, including **E** social novel index and **F** total distance traveled (cm) for each genotype and sex. **G** Correlations between time spent in the social/novel chamber (s) and time spent sniffing the social/novel mouse (s) were performed for each sex and genotype. Moreover, correlations between **H** social behavior and PFC 5-HT and tryp levels were accessed for (top) WT and (bottom) transgenic mice. The results are expressed as mean ± SEM ($n = 9$–12 **B, C, E–G,** $n = 6$–8 **H** for each group). *$p < 0.05$, **$p < 0.01$ by 2WAY ANOVA with Sidak's multiple comparisons-test **B, C, E, F**, Spearman's correlation (**H**, WT) and Pearsons's correlation (**G, H,** *Tsc2*$^{+/-}$).

social index: $p = 0.014$, $r = 0.90$; social novel index: $p = 0.04$, $r = 0.83$; Fig. 5H). Correlation analysis between social behavior and MRS data was also performed, but no significant correlations were found (Figure S1, Supplementary File).

DISCUSSION

Building on the hypothesis that sex-dependent changes in cortical morphology and neurophysiology contribute to distinct social impairments in males and females with ASD, we provide evidence that sexually dimorphic traits, ranging from cellular to neuronal circuit levels, may underlie network dysfunctions and the distinct social behavior patterns observed between sexes in ASD.

This study is the first to analyse basal and apical dendrite morphology in both males and females for the *Tsc2*$^{+/-}$ mice, a mouse model exhibiting both ASD-like behavior and increased excitability [30]. Our results suggest that transgenic males have a limited capacity to integrate information from local circuits within the cortical region, implied by shorter and less complex basal dendrites. In females, apical dendrites might have developed in a more complex and longer morphology that could be a compensatory mechanism to maintain or enhance neural connectivity in response to information from distant brain regions. Accordingly, data on ASD and epilepsy [18, 39–42], mostly obtained in males, reported the same alterations that we observed in *Tsc2*$^{+/-}$ males. These results unveil, for the first time, inherent sexual dimorphism in neuronal morphology within the context of ASD, potentially elucidating the pronounced sex differences in incidence and manifestations observed in this disorder. Dendritic spines are also an important aspect of neuronal morphology, strongly influencing neural network activity [43]. Another important finding of this work was that *Tsc2*$^{+/-}$ animals have increased mushroom and reduced thin dendritic spine density in cortical pyramidal neurons. In agreement, a study reported that sub-threshold synaptic stimulation and activation of the mammalian target of the rapamycin (mTORC1), which results from *Tsc2* gene mutation [44, 45], resulted in significant enlargement of spine heads, a sign of enhanced excitatory synapse formation [46]. However, for ASD an increase in spine densities with immature morphology has been described, indicating a general spine immaturity state [40, 47]. From our results we can postulate that in this mouse model spines were adapted as a result of increased neural activity to establish enhanced excitatory synapse formation. Since brain circuits are preserved through precise synaptic connections [16], these cortical morphological alterations observed could originate changes in cortical neuronal transmission.

Additionally, here, we demonstrated that transgenic mice exhibited reduced 5-HT$_{1A}$ receptor density that have been also described from neuroimaging and postmortem data in ASD patients [48–50]. In parallel, *Tsc2*$^{+/-}$ mice had higher cortical concentrations of glutamate which agree with elevation in glutamatergic activity previously reported for *Tsc2*$^{+/-}$ and ASD [30, 51]. Significantly, we found a female sex bias in those specific alterations as only *Tsc2*$^{+/-}$ females exhibited higher excitability but reduced 5-HT$_{1A}$ receptor density than their WT littermates. Importantly, it has been proposed that serotonin, acting on 5-HT$_{1A}$ receptors, suppresses glutamate release [52, 53]. Yet, in our transgenic mice, we showed that greater cortical 5-HT$_{1A}$ receptor density correlates with higher excitability. We argue that activation of 5-HT$_{1A}$ receptor could be a result from higher excitability in *Tsc2*$^{+/-}$ mice to compensate for that imbalance. However, from our results, that inhibitory effect was still insufficient to suppress glutamate release. From that, we postulate that serotonergic dysfunctions could be associated with the E/I imbalance shifted to excitability in this animal model and specifically for females. In addition, considering that GABA is unchanged this further supports a direct effect on glutamate transmission. Additionally, a sexual dimorphism in concentrations of tryp, a precursor of 5-HT, was also observed. Considering that *Tsc2*$^{+/-}$ females exhibited significantly lower receptor density but comparable tryp and 5-HT levels than their WT littermates, we proposed that the presynaptic input remains intact, and the observed effects in *Tsc2*$^{+/-}$ females are likely due to alterations in the postsynaptic 5-HT$_{1A}$ receptor density on glutamatergic neurons. The fact that increased excitability correlates with higher 5-HT$_{1A}$ receptor density in transgenic mice may reflect a dysregulation in the receptor signaling rather than a change in presynaptic function.

Alterations in both morphological and molecular signaling can disrupt the typical development of structural and functional neural networks [22]. Here, we also exposed that the TSC2 mouse model exhibited sex-dependent changes in structural connectivity, particularly in the cortex-amygdala-hippocampus circuit. Transgenic females showed a reduced number of axonal fiber pathways, while *Tsc2*$^{+/-}$ males displayed a loss of tissue density reflected by increased ADC values, both indicating reduced microstructural integrity of white matter tracts, which has been previously reported in TSC [54–57]. Regarding sex-specific alterations, a previous study including only male patients reported increased diffusion values [58], consistent with our findings in *Tsc2*$^{+/-}$ males. From our results, we propose that the sex-specific dysfunctions in neuronal morphology are directly linked to similar sex-dependent impairments in structural connectivity. In females, the reduced number of long-range axonal fibers (white matter tracts) likely affects axonal integrity and the neurons' ability to transmit signals across distant regions. That could be linked to the apical dendritic alterations observed specifically in females. In males, the loss of tissue density likely reflects a reduced concentration of cells and cellular structures, which may result from smaller and less complex neurons reported in males. Importantly, the cortex-amygdala-hippocampus network is often implicated in social and cognitive impairments, emotional dysregulation, and stress-related disorders [23–26]. We believe that these sex-related network impairments may partially explain the sexually dimorphic symptoms in tuberous sclerosis complex (TSC) and related clinical manifestations, such as ASD [59].

Social interaction and communication deficits are widely recognised as one of the core ASD features [60], which are also observed in our animal model. In parallel, consistent research also suggests that there are significant differences between genders in people diagnosed with ASD [5, 61]. Our study indicated that *Tsc2*$^{+/-}$ females had reduced sociability. We believe that exposure to a non-familiar animal for the first time could generate a more anxious condition in transgenic females, leading them to avoid social interaction. In a previous work, we hypothesized that social impairment in female *Tsc2*$^{+/-}$ mice might represent a stress-coping strategy [30], potentially linked to the higher social anxiety observed in females, which is often associated with camouflaging behavior [5, 62]. On the other hand, only transgenic males showed increased locomotion and lower social novelty preference compared with their WT littermates, which agrees with previous work in other ASD mouse model [5]. Moreover, the transgenic males were the experimental group that faced more difficulties during close social interaction from the social novelty test phase. Interestingly, the females of our animal model resemble girls' ability to camouflage their autistic traits seen in humans [5], since *Tcs2*$^{+/-}$ females presented "normative" social patterns upon familiarisation. Importantly, for the first time, our data proved that cortical serotoninergic metabolism strongly correlates with social deficits in *Tcs2*$^{+/-}$ mice. We showed that animals with higher cortical 5-HT and tryp concentrations had more developed social skills. This finding is aligned with previous studies indicating that systemic enhancement of the serotoninergic system reverses social deficits in multiple mouse models for ASD [13] and that increasing dietary tryp intake ameliorated autism symptoms [63].

It has been suggested that TSC-related neural alterations may underlie its clinical manifestations, potentially linking

disruptions in cellular and circuit signaling to the development of neurological and neuropsychiatric symptoms, such as ASD and cognitive/intellectual impairments [22, 55, 64]. Interestingly, our study exposed that, similar to social deficits, structural connectivity alterations reflect dysfunctional network communication, though in distinct domains. Females exhibit a reduced number of white matter fibers within the network, while in males, the number of fibers remains unchanged, but their density is significantly reduced. This evidence suggests that the number of fibers may play a more primordial role in sociability—impaired in females—whereas fiber density may act as a secondary player influencing novel social interactions, as seen in males. Moreover, we propose that these sex-dependent impairments in structural connectivity result from sex-specific dysfunctions in neuronal morphology. Notably, altered 5-HT_{1A} receptor density and hyperexcitability, which likely reflect compromised communication between excitatory (glutamatergic) neurons, were observed exclusively in females. From that we believe that both E/I balance and 5-HTergic have a greater impact on sociability rather than on novel social interactions, further highlighting the sexually dimorphic nature of these disruptions. Moreover, based on our results, tryp supplementation may offer a potential therapeutic strategy to address social deficits, an approach that has also garnered interest for other psychiatric and neurological disorders associated with disruptions in tryp and 5-HT metabolism [65]. Our findings further imply that while the core symptoms of ASD may appear similar, the pathways leading to these symptoms can vary significantly between sexes. This insight underscores the importance of considering sex as a critical factor in both the study and treatment of ASD.

DATA AVAILABILITY

Data and materials will be made available on request.

REFERENCES

1. American Psychiatric Association. Diagnostic and statistical manual of mental disorders (5th ed.). American Psychiatric Association (2013).
2. Maenner MJ, Warren Z, Williams AR, Amoakohene E, Bakian AV, Bilder DA, et al. Prevalence and characteristics of autism spectrum disorder among children aged 8 years — autism and developmental disabilities monitoring network, 11 sites, United States, 2020. MMWR Surveill Summ. 2023;72:1–14.
3. Cruz S, Zubizarreta SC-P, Costa AD, Araújo R, Martinho J, Tubío-Fungueiriño M, et al. Is there a bias towards males in the diagnosis of autism? A systematic review and meta-analysis. Neuropsychol Rev. 2024;35:153–76.
4. Wood-Downie H, Wong B, Kovshoff H, Cortese S, Hadwin JA. Research review: a systematic review and meta-analysis of sex/gender differences in social interaction and communication in autistic and nonautistic children and adolescents. J Child Psychol Psychiatry. 2021;62:922–36.
5. Santos S, Martins B, Sereno J, Martins J, Castelo-Branco M, Gonçalves J. Neurobehavioral sex-related differences in Nf1+/− mice: female show a "camouflaging"-type behavior. Biol Sex Differ. 2023;24:1–14.
6. Rubenstein JLR, Merzenich MM. Model of autism: increased ratio of excitation/inhibition in key neural systems. Genes, Brain Behav. 2003;2:255–67.
7. Sohal VS, Rubenstein JLR. Excitation-inhibition balance as a framework for investigating mechanisms in neuropsychiatric disorders. Mol Psychiatry. 2019;24:1248–57.
8. Port RG, Oberman LM, Roberts TP. Revisiting the excitation/inhibition imbalance hypothesis of ASD through a clinical lens. Br J Radiol. 2019;92:20180944.
9. Gonçalves J, Violante IR, Sereno J, Leitão RA, Cai Y, Abrunhosa A, et al. Testing the excitation/inhibition imbalance hypothesis in a mouse model of the autism spectrum disorder: in vivo neurospectroscopy and molecular evidence for regional phenotypes. Mol Autism. 2017;8:1–8.
10. Yizhar O, Fenno LE, Prigge M, Schneider F, Davidson TJ, O'Shea DJ, et al. Neocortical excitation/inhibition balance in information processing and social dysfunction. Nature. 2011;477:171–8.
11. Kiser D, SteemerS B, Branchi I, Homberg JR. The reciprocal interaction between serotonin and social behaviour. Neurosci Biobehav Rev. 2012;36:786–98.
12. Branchi I. The double edged sword of neural plasticity: increasing serotonin levels leads to both greater vulnerability to depression and improved capacity to recover. Psychoneuroendocrinology. 2011;36:339–51.
13. Walsh JJ, Llorach P, Cardozo Pinto DF, Wenderski W, Christoffel DJ, Salgado JS, et al. Systemic enhancement of serotonin signaling reverses social deficits in multiple mouse models for ASD. Neuropsychopharmacology. 2021;46:2000–10.
14. Thorne BN, Ellenbroek BA, Day DJ. The serotonin reuptake transporter modulates mitochondrial copy number and mitochondrial respiratory complex gene expression in the frontal cortex and cerebellum in a sexually dimorphic manner. J Neurosci Res. 2022;100:869–79.
15. Poceviciute I, Kasperaviciute K, Buisas R, Ruksenas O, Vengeliene V. Sex differences in serotonergic control of rat social behaviour. Pharmacol Biochem Behav. 2023;223:173533.
16. Mueller-Buehl C, Wegrzyn D, Bauch J, Faissner A. Regulation of the E/I-balance by the neural matrisome. Front Mol Neurosci. 2023;16:1102334.
17. Kraus C, Castrén E, Kasper S, Lanzenberger R. Serotonin and neuroplasticity – links between molecular, functional and structural pathophysiology in depression. Neurosci Biobehav Rev. 2017;77:317–26.
18. Rossini L, de Santis D, Mauceri RR, Tesoriero C, Bentivoglio M, Maderna E, et al. Dendritic pathology, spine loss and synaptic reorganization in human cortex from epilepsy patients. Brain. 2021;144:251–65.
19. Akhgari A, Michel TM, Vafaee MS. Dendritic spines and their role in the pathogenesis of neurodevelopmental and neurological disorders. Rev Neurosci. 2024;35:489–502.
20. Nelson AD, Bender KJ. Dendritic integration dysfunction in neurodevelopmental disorders. Dev Neurosci. 2021;43:201–21.
21. Spruston N. Pyramidal neurons: dendritic structure and synaptic integration. Nat Rev Neurosci. 2008;9:206–21.
22. Shephard E, McEwen FS, Earnest T, Friedrich N, Mörtl I, Liang H, et al. Oscillatory neural network alterations in young people with tuberous sclerosis complex and associations with co-occurring symptoms of autism spectrum disorder and attention-deficit/hyperactivity disorder. Cortex. 2022;146:50–65.
23. Sumiya M, Okamoto Y, Koike T, Tanigawa T, Okazawa H, Kosaka H, et al. Attenuated activation of the anterior rostral medial prefrontal cortex on self-relevant social reward processing in individuals with autism spectrum disorder. Neuroimage Clin. 2020;26:102249.
24. Mohapatra AN, Wagner S. The role of the prefrontal cortex in social interactions of animal models and the implications for autism spectrum disorder. Front Psychiatry. 2023;14:1205199.
25. Misra V. The social brain network and autism. Ann Neurosci. 2014;21:69–73.
26. Godsil BP, Kiss JP, Spedding M, Jay TM. The hippocampal–prefrontal pathway: the weak link in psychiatric disorders? Eur Neuropsychopharmacol. 2013;23:1165–81.
27. Lu H, song Liu Q. Serotonin in the frontal cortex: a potential therapeutic target for neurological disorders. Biochem Pharmacol. 2017;6:e184.
28. Albert PR, Vahid-Ansari F, Luckhart C. Serotonin-prefrontal cortical circuitry in anxiety and depression phenotypes: pivotal role of pre- and post-synaptic 5-HT1A receptor expression. Front Behav Neurosci. 2014;8:199.
29. Caballero A, Orozco A, Tseng KY. Developmental regulation of excitatory-inhibitory synaptic balance in the prefrontal cortex during adolescence. Semin Cell Dev Biol. 2021;118:60–3.
30. Ferreira H, Sousa AC, Sereno J, Martins J, Castelo-Branco M, Gonçalves J. Sex-dependent social and repetitive behavior and neurochemical profile in mouse model of autism spectrum disorder. Metabolites. 2022;12:1–15.
31. Crespo P, Blanco A, Couceiro M, Ferreira NC, Lopes L, Martins P, et al. Resistive plate chambers in positron emission tomography. Eur Phys J Plus. 2013;128:1–35.
32. Provencher SW. Automatic quantitation of localized in vivo 1 H spectra with LCModel. NMR Biomed. 2001;14:260–4.
33. Tropea D, Harkin A. Biology of brain disorders. Tropea D, Harkin A, editors. Front Cell Neurosci. 2017;11:366.
34. Krasikova RN, Andersson J, Truong P, Nag S, Shchukin EV, Halldin C.A fully automated one-pot synthesis of [carbonyl-11C]WAY-100635 for clinical PET applications.Appl Radiat Isot. 2009;67:73–8.
35. Mirrione MM, Schiffer WK, Fowler JS, Alexoff DL, Dewey SL, Tsirka SE. A novel approach for imaging brain–behavior relationships in mice reveals unexpected metabolic patterns during seizures in the absence of tissue plasminogen activator. Neuroimage. 2007;38:34–42.
36. Carla F, Susana C, Ricardo F, Mariana LP, Joana G, Antoni C, et al. Cannabinoid modulation of monoamine levels in mouse brain: unveiling neurochemical dynamics through an innovative high-performance liquid chromatography-fluorescence detection bioanalysis. J Anal Test. 2024;8:300–14.
37. Kaidanovich-Beilin O, Lipina T, Vukobradovic I, Roder J, Woodgett JR. Assessment of social interaction behaviors. J Vis Exp. 2011;48:2473.
38. Charan J, Kantharia ND. How to calculate sample size in animal studies? J Pharmacol Pharmacother. 2013;4:303.

39. Mukaetova-Ladinska EB, Arnold H, Jaros E, Perry R, Perry E. Depletion of MAP2 expression and laminar cytoarchitectonic changes in dorsolateral prefrontal cortex in adult autistic individuals. Neuropathol Appl Neurobiol. 2004;30:615–23.
40. Martínez-Cerdeño V. Dendrite and spine modifications in autism and related neurodevelopmental disorders in patients and animal models. Dev Neurobiol. 2017;77:393–404.
41. Barón-Mendoza I, Del Moral-Sánchez I, Martínez-Marcial M, García O, Garzón-Cortés D, González-Arenas A. Dendritic complexity in prefrontal cortex and hippocampus of the autistic-like mice C58/J. Neurosci Lett. 2019;703:149–55.
42. Swann JW, Al-Noori S, Jiang M, Lee CL. Spine loss and other dendritic abnormalities in epilepsy. Hippocampus. 2000;10:617–25.
43. Jean G, Carton J, Haq K, Musto AE. The role of dendritic spines in epileptogenesis. Front Cell Neurosci. 2023;17:1173694.
44. Feliciano DM, Lin TV, Hartman NW, Bartley CM, Kubera C, Hsieh L, et al. A circuitry and biochemical basis for tuberous sclerosis symptoms: from epilepsy to neurocognitive deficits. Int J Dev Neurosci. 2013;31:667–78.
45. Connolly MB, Hendson G, Steinbok P. Tuberous sclerosis complex: a review of the management of epilepsy with emphasis on surgical aspects. Childs Nerv Syst. 2006;22:896–908.
46. Henry FE, Hockeimer W, Chen A, Mysore SP, Sutton MA. Mechanistic target of rapamycin is necessary for changes in dendritic spine morphology associated with long-term potentiation. Mol Brain. 2017;10:50.
47. Barón-Mendoza I, Maqueda-Martínez E, Martínez-Marcial M, De la Fuente-Granada M, Gómez-Chavarin M, González-Arenas A. Changes in the number and morphology of dendritic spines in the hippocampus and prefrontal cortex of the C58/J mouse model of autism. Front Cell Neurosci. 2021;15:726501.
48. Oblak A, Gibbs TT, Blatt GJ. Reduced serotonin receptor subtypes in a limbic and a neocortical region in autism. Autism Res. 2013;6:571–83.
49. Goldberg J, Anderson GM, Zwaigenbaum L, Hall GBC, Nahmias C, Thompson A, et al. Cortical serotonin type-2 receptor density in parents of children with autism spectrum disorders. J Autism Dev Disord. 2009;39:97–104.
50. Murphy DGM, Daly E, Schmitz N, Toal F, Murphy K, Curran S, et al. Cortical serotonin 5-HT 2A receptor binding and social communication in adults with Asperger's syndrome: an in vivo SPECT study. Am J Psychiatry. 2006;163:934–6.
51. Manyukhina VO, Prokofyev AO, Galuta IA, Goiaeva DE, Obukhova TS, Schneiderman JF, et al. Globally elevated excitation–inhibition ratio in children with autism spectrum disorder and below-average intelligence. Mol Autism. 2022;13:20.
52. Matsuyama S, Nei K, Tanaka C. Regulation of glutamate release via NMDA and 5-HT1A receptors in guinea pig dentate gyrus. Brain Res. 1996;728:175–80.
53. Ostrowski TD, Ostrowski D, Hasser EM, Kline DD. Depressed GABA and glutamate synaptic signaling by 5-HT 1A receptors in the nucleus tractus solitarii and their role in cardiorespiratory function. J Neurophysiol. 2014;111:2493–504.
54. Tsai J-D, Ho M-C, Lee H-Y, Shen C-Y, Li J-Y, Weng J-C. Disrupted white matter connectivity and organization of brain structural connectomes in tuberous sclerosis complex patients with neuropsychiatric disorders using diffusion tensor imaging. Magn Reson Mater Physics, Biol Med. 2021;34:189–200.
55. Scherrer B, Prohl AK, Taquet M, Kapur K, Peters JM, Tomas-Fernandez X, et al. The connectivity fingerprint of the fusiform gyrus captures the risk of developing autism in infants with tuberous sclerosis complex. Cereb Cortex. 2020;30:2199–214.
56. Im K, Ahtam B, Haehn D, Peters JM, Warfield SK, Sahin M, et al. Altered structural brain networks in tuberous sclerosis complex. Cereb Cortex. 2016;26:2046–58.
57. Hsieh CC, Lo Y-C, Wang H-H, Shen H-Y, Chen Y-Y, Lee Y-C. Amelioration of the brain structural connectivity is accompanied with changes of gut microbiota in a tuberous sclerosis complex mouse model. Transl Psychiatry. 2024;14:68.
58. Baumer FM, Song JW, Mitchell PD, Pienaar R, Sahin M, Grant PE, et al. Longitudinal changes in diffusion properties in white matter pathways of children with tuberous sclerosis complex. Pediatr Neurol. 2015;52:615–23.
59. Ryu JH, Sykes A-MG, Lee AS, Burger CD. Cystic lung disease is not uncommon in men with tuberous sclerosis complex. Respir Med. 2012;106:1586–90.
60. Costescu C, Pitariu D, David C, Rosan A. social communication predictors in autism spectrum disorder. theoretical review. J Exp Psychopathol. 2022;13:204380872211069.
61. Allen K-A, Boyle C, Lauchlan F, Craig H. Using social skills training to enhance inclusion for students with ASD in mainstream schools. Inclusive Education: Global Issues and Controversies. BRILL; 2020. p. 202–15.
62. Alaghband-rad J, Hajikarim-Hamedani A, Motamed M. Camouflage and masking behavior in adult autism. Front Psychiatry. 2023;14:1108110.
63. Beretich GR. Reversal of autistic symptoms by removal of low-relative tryptophan foods: case report. Med Hypotheses. 2009;73:856–7. Churchill Livingstone
64. Bassetti D, Luhmann HJ, Kirischuk S. Effects of mutations in TSC genes on neurodevelopment and synaptic transmission. Int J Mol Sci. 2021;22:7273.
65. Pais ML, Martins J, Castelo-Branco M, Gonçalves J. Sex differences in tryptophan metabolism: a systematic review focused on neuropsychiatric disorders. Int J Mol Sci. 2023;24:6010.

AUTHOR CONTRIBUTIONS

MLP, MCB and JG designed the study; MLP acquired behavioral and Golgi staining data; CS did the manual quantification of the total time sniffing; JS acquired DTI data and MLP and JS acquired MRS and PET/MRI data; VAT performed the radiochemical production of [carbonyl-^{11}C]WAY-100635; MLP and CF acquired HPLC data; MLP processed and analysed all data; MLP wrote the paper; JG and MCB supervised the project; LP supervised neuronal morphology task and validated neuronal morphology data analysis; AF supervised HPLC task and validated HPLC data analysis; all authors contributed to interpreting data and writing and editing of the manuscript. All authors read and approved the final manuscript.

FUNDING

This work was supported by Ph.D. Fellow 2020.06582.BD (https://doi.org/10.54499/2020.06582.BD), Ph.D. Fellow 2021.06135.BD (https://doi.org/10.54499/2021.06135.BD), FCT Exploratory Project 2022.01066.PTDC and Strategic Plan FCT/UIDP&B/04950/2025, COMPETE and FEDER funds, FCT, Portugal and ICNAS Pharma Unipessoal, Lda.

COMPETING INTERESTS

The authors declare no competing interests.

ADDITIONAL INFORMATION

Supplementary information The online version contains supplementary material available at https://doi.org/10.1038/s41398-025-03464-7.

Correspondence and requests for materials should be addressed to Joana Gonçalves.

Reprints and permission information is available at http://www.nature.com/reprints

Publisher's note Springer Nature remains neutral with regard to jurisdictional claims in published maps and institutional affiliations.